Article

The Physicochemical Method Uses Industrial Leftover Hemp Fibre Cellulose to Make Micron-Sized Hemp Powder

Sarker Md Shamim , Yonghe Huan , Linli Gan , Shangyong Zhang *

Posted Date: 28 December 2023

doi: 10.20944/preprints202312.2166.v1

Keywords: leftover hemp fibre recycling process, chemical treatment with cellulose, making a micron-sized powder, average particle size

Article

The Physicochemical Method Uses Industrial Leftover Hemp Fibre Cellulose to Make Micron-Sized Hemp Powder

Sarker Md Shamim [1,2], Yonghe Huan [1], Linli Gan [1,2] and Shangyong Zhang [1,*]

[1] Wuhan Textile University, School of Textile Science and Engineering, Wuhan, China, No.1 Sunshine Avenue, Jiangxia District, Wuhan 430200, China; ssharker525@gmail.com (S.M.S); 2903423518@qq.com (Y.H); 1247690340@gg.com (L.G); 1989029@wtu.edu.cn (S.Z)

[2] State Key Laboratory of New Textile Materials and Advanced Processing Technologies, Wuhan, China, No.1 Sunshine Avenue, Jiangxi District, Wuhan 430200, China

* Correspondence: Corresponding author e-mail: 1989029@wtu.edu.cn

Abstract: One of the most widely available and extensively produced varieties of industrial hemp, which generates a substantial amount of consumer-increasing waste in the form of hemp cellulose. In this study, recycling with a compressed and high-speed method that combines crushing and alkali treatment effectively converts leftover hemp fiber into ultrafine powder. The SEM (Scanning Electron Microscopy), AFM (Atomic Force Microscope), FTIR (Fourier-transform Infrared Spectroscopy), and XRD (X-ray Diffraction) examined the original morphology of hemp fiber treated with alkali, fiber heated to 200 ℃, and crushed powder. Particle size, crystallinity, fiber surface, and strength increased and decreased. It became apparent that fiber strength decreased, and fiber roughness significantly increased after alkali treatment. Fiber increased significantly, and crystallinity decreased after crushing. It was simple and effective for converting the leftover hemp fiber into micron-sized powder. In about 3 to 5 minutes, approximately 1 kg of dry ultrafine powder with a particle size of 10.44μm was produced. This production method will significantly enhance future industrial applications of waste hemp fiber.

Keywords: leftover hemp fibre recycling process; chemical treatment with cellulose; making a micron-sized powder; average particle size

1. Introduction

Worldwide production indicates a range of 32,140 ha to 142,883 tonnes, resulting in an average yield of 4.45 tonnes ha^{-1} [1]. Extensive regional cultivation ranges and various uses. The top three countries by production area for hemp production, according to FAO Stat (2018), are North Korea (21,247 ha), France (12,900 ha), and Canada (555,853 ha) [3] In 2019, the industrial hemp market is expected to be valued at USD 4.71 billion worldwide [2]. Currently, more than 30 countries are involved in the Global Hemp Trade, and almost 651 tons fall within the legal framework for cannabis and textile consumption. Rapid product growth generates millions of tons of textile waste annually [3]. Studying the percentage of short fibers in hemp fiber, which are often removed during the production of hemp yarn and fabric, is one method. Notably, Hemp Fiber has a short Fiber, hemp stalk, and yield, with a percentage of roughly 7.72%,40%, and 60% waste. Moreover, the rate of total waste from opening to spinning can range from 8.5% to 18%. Considerable destruction of natural resources has resulted in significant financial losses as well. Furthermore, it causes environmental issues such as water and soil pollution [4,5]. There are concerns about these severe circumstances worldwide. Because of this, it must be addressed effectively and efficiently. Utilize leftover cellulose polysaccharide fibers to create a valuable product [6,7]. The textile industry would have enormous revenue potential if these waste fibers could be recycled [8].

Hemp waste recycling techniques can be broadly classified into physical and chemical methods. Particle technology was considered a topic worthy of independent study before the mid- 1960s [9]. It

 doi:10.20944/preprints202312.2166.v1

became apparent that the materials displayed certain modifications after being processed into an ultrafine powder, including surface area, surface energy, activity, and interface characteristics [10,11]. Possessing an in-depth knowledge of ultra-fine particles and their properties, ultrafine powder has been the focus of processing equipment development. It is widely utilized in various industrial fields, including composite materials, chemicals, biology, catalysis, and medicine, demonstrating extensive applications [12,13]. Hemp ultrafine powder is used for reinforcing composites; hemp fibers have several advantages over synthetic fibers and can be effectively employed in many applications[14], such as biofuel, agricultural, animal bedding, industrial and automotive, bridgeable plastics, textile, paper, construction material, food, beverage, cosmetic and personal care products. The macromolecular polysaccharide hemp cellulose comprises β-1, 4 glycosidic linkages, and D-glucose. It is a type of covalent bond. Three components contribute to the high chemical reactivity of cellulose, a polysaccharide hydroxyl group – OH [2]. According to their chemical solid bonds, orientation, crystallinity, and high levels of polymerization, producing ultrafine powders from leftover hemp fibers is difficult. There are two ways to make cellulose powders: mechanical and chemical [15]. Toxic and complex chemicals are usually used in chemical reactions that produce fine powder [16,17]. A few research investigations have been made on mechanical and chemical milling of wool and silk powder [13,18]. The cotton and wool powder with a particle size of around 60μm and 40μm were produced using freeze-milling and millstone milling techniques. The processing of the fibre into dry powder for 1 kilogram took approximately 1.5 hours[8,15].

In this work, hemp fibres were first treated with acid to affect their morphology and make it easier for them to break into an effective powder before they were crushed. Ultimately, after 3 to 5 minutes, roughly 1 kg of dry powder with a particle size of about 10.44μm was produced. This approach's dry ultrafine hemp crushed powder output and efficiency were significantly higher than ball milling, cutting milling, bead milling, millstone, and spray drying techniques. This method has a lot of potential for future production utilization.

2. Experiment

2.1. Materials

Wasted hemp fiber from Wuhan Hemp Biological Technology Co., Ltd, and Sulfuric acid (H_2SO_4) from Wuhan Jiangbei Chemical Reagent Co., ltd. The XL-06B mixer and refining agent YK were purchased from Kekai Fine Chemical Shanghai Co., Ltd, China. Ethanol absolute (C2H6O) was purchased from Sinopharm Chemical Reagent Co., Ltd.

2.2. Acid Treatment and Modification of hemp Fiber

First, place a beaker containing 200 ml of boiled deionized water into 100°C water baths for. Then, 2 g/L sulfuric acid raw material, 1 g/L YK agent, and 10 gm of leftover untreated hemp fiber were (cut to 2 mm × 3 mm) were sequentially added to the beaker. The bath ratio was 1:20. After heating the beaker for 1 hour, wash the hemp fiber 7–8 times because the YK agent creates more foam, and the pH value was 7. Next, use a padding machine or hand roller to remove excess water. Finally, hemp fiber was placed in the oven and baked at 200 °C for 1 hour. On the other hand, the powder was prepared for AFM to be dissolved using C2H6O at 39.82 g/L and hemp powder at 0.70 g/L for 30 minutes. The acid modification process illustrated in Figure 3(b)

2.3. Modified Hemp Fiber on a Crusher Efficiently

Firstly, hemp cellulose was cut from 2 mm to 3 mm, and small scissors were used before chemical treatment. About 1 kg of modified hemp fiber with a short length was used in a small Chinese Medicine crusher XL-06B (Aashia Company, China). It has a high-quality lid with 3 blades: the 1-crushing blade, which helps to crush fiber, is enormous and the 2-bottom slight edge is for grinding hemp cellulose, while the 3-cutter head cuts yarn into small pieces. It has a power of 1100 watts, a voltage of 220 volts, a fineness of 200, and a speed of 25000 revolutions per minute. By running at

Preprints (www.preprints.org) | NOT PEER-REVIEWED | Posted: 28 December 2023 doi:10.20944/preprints202312.2166.v1

high capacity, hemp cellulose was broken. As a process, it took 3 to 5 min to crush around 1 kg of ultrafine hemp powder. The crusher instruction manual appears in Figure 1.

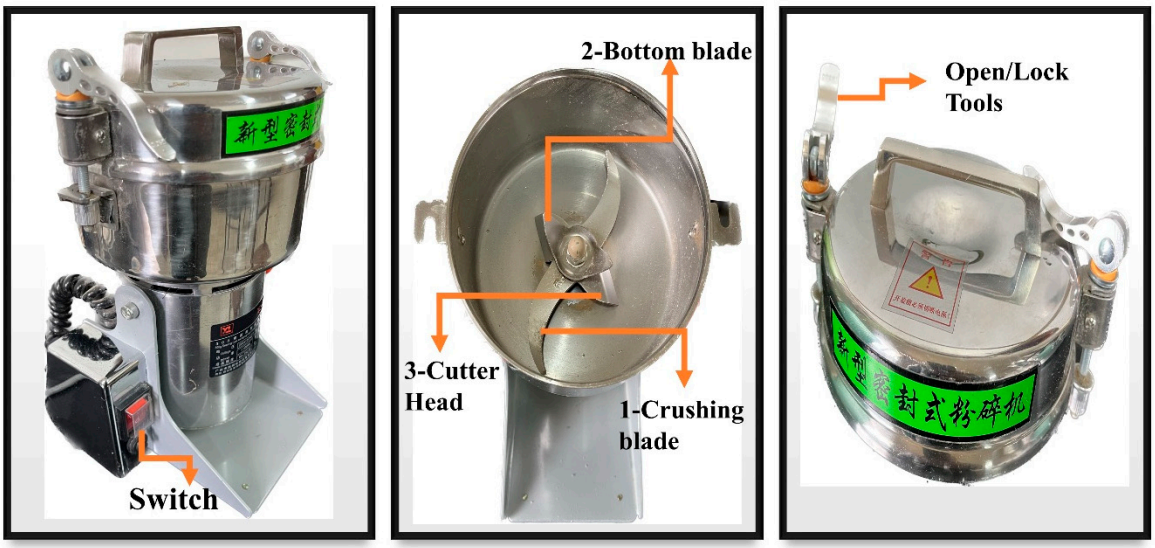

Figure 1. Crusher instruction Manual.

2.4. Characterization

Utilizing a scanning electron microscope (SEM, JSM-7800, Japan Electronics, Tokyo, Japan), the morphology of hemp fiber, following its coating with gold powder, was examined. An accelerating voltage of 5 kV and a magnification of 5000 times were used.

The surface roughness of hemp fiber and powder was measured before and after acid treatment using an atomic force microscope (AFM, model number SPM-9700 Shimazu, Japan). The process involved converting hemp powder into a liquid using ethanol (C2H6O) for 30 minutes. A scanning area of 5μm × 5μm with a 2×2,μm^2 zoom was used to measure each sample.

Fourier-transform infrared spectroscopy (FTIR; type IRT Racer-100; Kyoto, Japan; SHIMADZU CORPORATION) 4 cm^{-1} was used for spectral resolution. The samples were analyzed in the nitrogen atmosphere using the Total Reflectance (ATR) mode. Forty scans were performed on each piece.

After treatment and milling, the hemp fiber was subjected to an X-ray diffraction (XRD) study using an X' Part Pro MPD (PA Analytical, Almelo, The Netherlands) to determine if there was a crystalline alteration. The theta testing range was 0°C–40°C, and the scan rate was 5 °C / min. The degree of crystallinity in a sample is determined by the crystallinity index (CI) [19].

$$CI(\%)=\frac{(I_{200}-I_{am})}{I_{200}}\times 100 \quad (1)$$

where I_{am} is the minimal peak intensity of the amorphous phase at about 17.1°, and I_{200} is the peak at 2θ angle intensity of the crystalline phase at about 22.5°.

3. Result and Discussion

3.1. Change in the Morphology of Hemp Fiber Before and After Crushing

The SEM images shown in Figure 4(a-h) depict OHF, MHF, THF, and HP, demonstrating modified hemp fiber surfaces after acid, temperature, and powder treatments. The process was highly magnified. Figure 4(a) shows that the original hemp fiber surface was slightly uneven compared to the acid treatment. Figure 4 (b) After the rougher alkali treatment surface, the strip gully was bigger and breakable. Concentration sulfuric acid can effectively penetrate the cellulose structure, destroy the orderly accumulation of molecular chains, and break the hydrogen bonds

Preprints (www.preprints.org) | NOT PEER-REVIEWED | Posted: 28 December 2023 doi:10.20944/preprints202312.2166.v1

inside cellulose [20]. Figure 4(c) After treatment with 200°C high temperatures and acid, fiber surfaces are weaker and more fragile. However, the texture of the etched hemp fiber surface differed from the appearance of the original hemp fiber surface. On the other hand, in Figure 4 (e-h), the low magnification picture OHF (a) appears smoother than that of the MHF(e) and THF(g). This effect demonstrated how light scattering at various levels on a uniform fiber surface altered the fiber's luster [21]. In Figure 4 (d-h), there were more imperfections and uneven edges on the crushed powder surface than on the fiber. Dry hemp fiber material is ground more finely. Generally, as particles become finer, the particle shape tends to be rectangular and more uniform [22]. Since untreated hemp fiber cannot be ground using the method of this study to make a fine powder, there is no original hemp powder sample for SEM image comparison.

a

$$\text{Cellulose} + H_2SO_4 \rightarrow \text{Nanocellulose} + H_2O$$

Figure 2. Hydrolysis reaction.

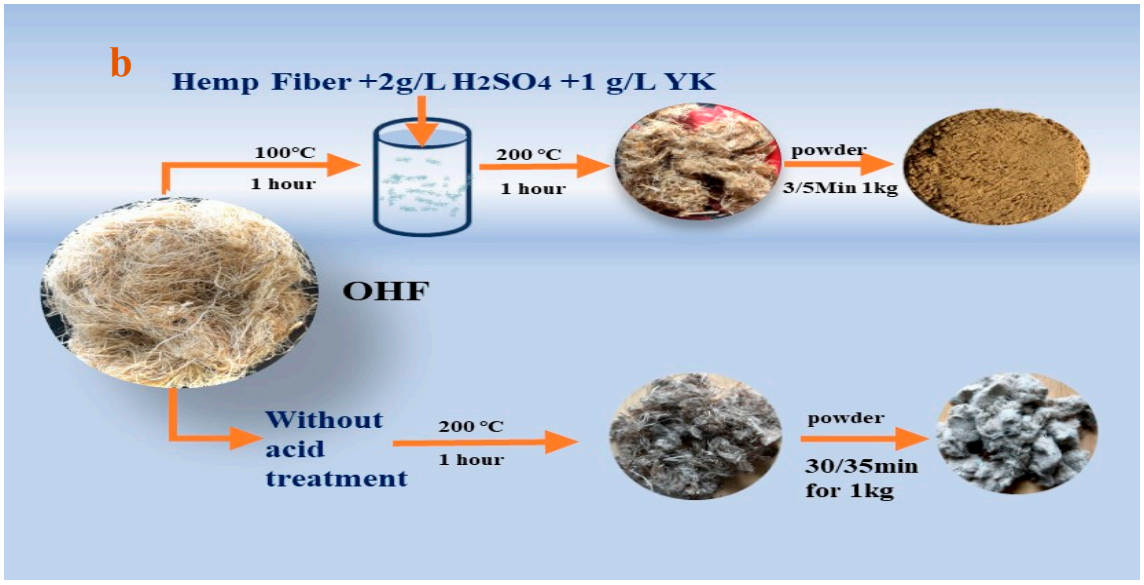

Figure 3. The process makes a powder without the acid test and with the acid test.

Preprints (www.preprints.org) | NOT PEER-REVIEWED | Posted: 28 December 2023 doi:10.20944/preprints202312.2166.v1

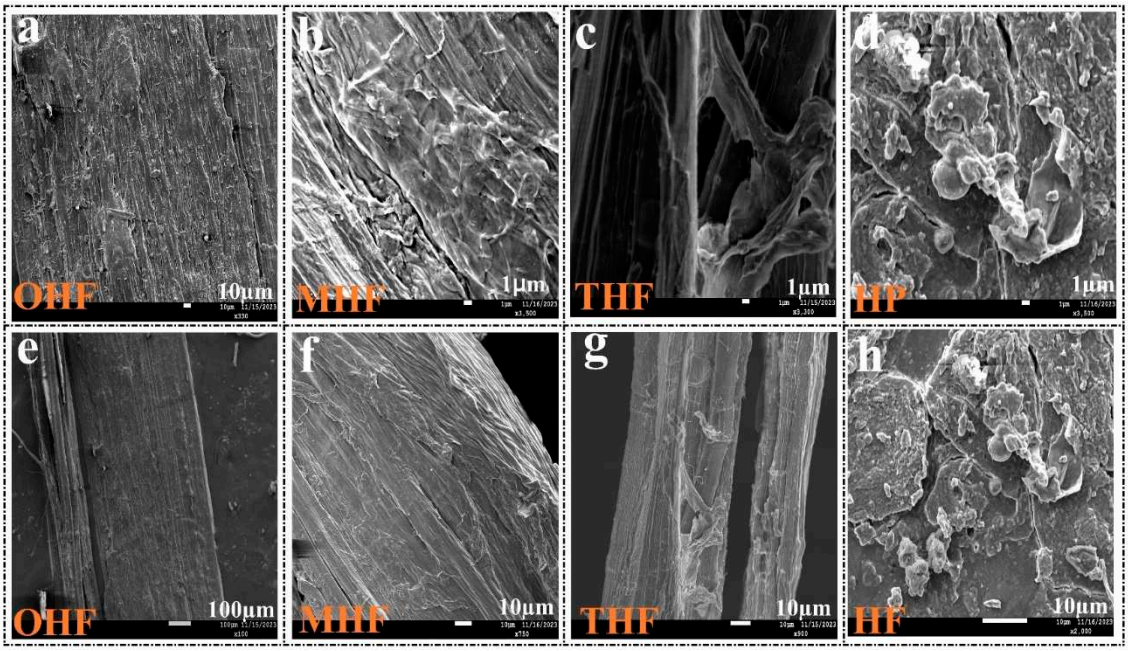

Figure 4. High magnification of (a)original hemp fiber OHF, (b)modified hemp fiber MHF, (c)temperature hemp fiber THF, (d) hemp powder HP, and low magnification (e)OHF, (f)MHF, (g)THF, (h)HP .

3.2. Surface Roughness of Hemp Morphology After Treatment and Crushing

Three-dimensional (3D) AFM pictures of hemp fibers at various temperatures and powders are displayed in Figure 5 (a–h). The surface features bumps, and there is an uneven distribution for every sample. Here, the result of the surface roughness total area for (a-e) OHF at 25μm is Ra: 270.365nm, Rz: 1.30μm, Rp: 615.901nm, and the scanning scale was 5μm × 5μm. The results can still be used as a reference when comparing various samples on the same scanning scale because they display layers of unevenness in different models. After chemical treatment (b-f) MHF, Ra, Rz, Rp was 109.491nm, 846.889μm, 423.870nm, showing orderly minimum roughness, and here the Ra value decreases. This indicates that the extensions' heights were significantly more consistent than those of OHF, THF, and HP. Sulfuric acid could dissolve lignin, hemicellulose, and pectin, among other non-cellulosic fiber components. The cellulose fiber in hemp was hydrolyzed and oxidized by sulfuric acid [23]. This may influence the fibers' mechanical and physical properties, such as stiffness, strength, fineness, and moisture absorption. Hydrolysis can decrease the fiber diameter of [24]. (c-g) THF, after 200℃, fiber roughness increased. Ra, Rz, Rp were orderly 125.854nm, 1.33μm, 686.299nm. Fiber surface roughness can be affected by temperature [25]. (d-h) HP had orderly Ra, Rz, Rp of 376.507nm, 2.692μm, 1.483nm. Therefore, upon etching, the degree of cellulose surface cracking was identical, and the cellulose surface's protuberance height tended to be more homologous than that of OHF. On the other hand, the HP had the highest roughness (d-h) because of The High-speed operation using different kinds of blade-focused powders, which were randomly sheared and crushed in various directions [26]. It was hard to ensure uniform crushing of each point on the surface of the powder [26,27].

Preprints (www.preprints.org) | NOT PEER-REVIEWED | Posted: 28 December 2023 doi:10.20944/preprints202312.2166.v1

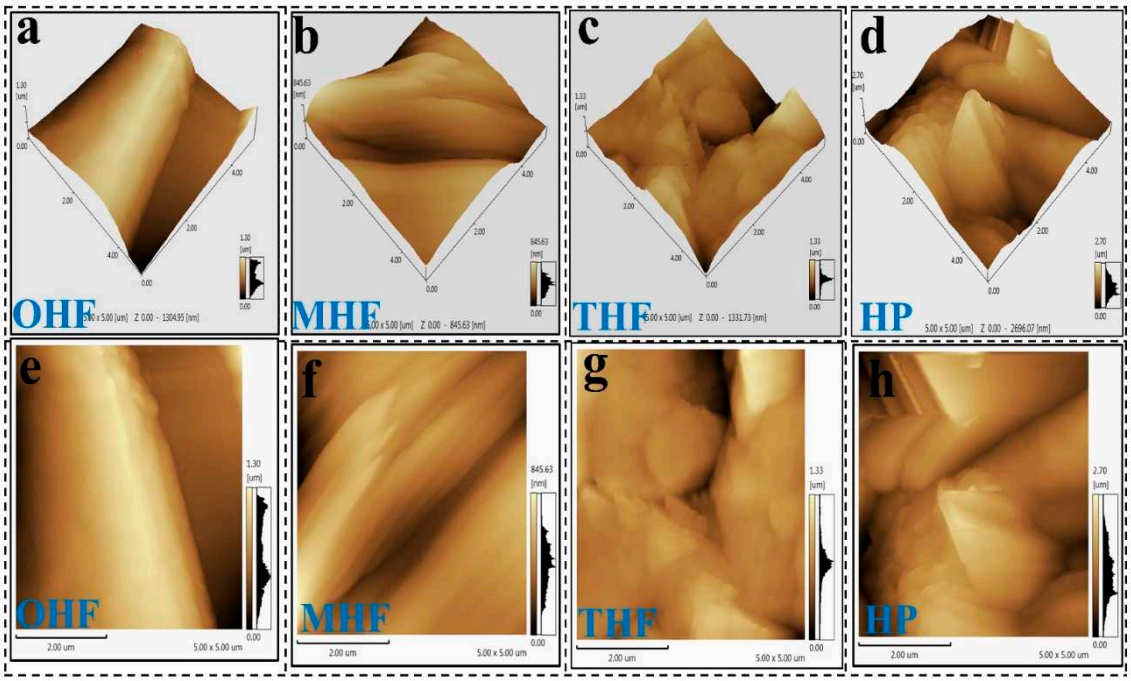

Figure 5. 5μm×5μm AFM scanning images of (a) original hemp fiber OHF (b) modified hemp fiber MHF (c)temperature hemp fiber THF (d) hemp powder HP, And (e)OHF (f)MHF (g)THF (h)HP.

3.3. Using the Crusher Effect as a Basis Analyze the Strength Loss of Modified Hemp Fiber

Extraction of modified hemp fiber using a single fiber strength tester proved difficult due to its significant strength loss and breakability during 200°C and alkali treatment. It has a clear appearance in SEM Figure 4 MHF, THF fibers are more fragile. Therefore, acid-containing and non-acid-containing fibers underwent both treatments and were combined using the same crusher to make a powder. It can be shown in Figure 3 (b). After the alkali treatment and high temperature, the original gray hemp fiber turns brown, and without acid, it looks like ash black. So, the alkali treatment process essentially destroys the strength of the hemp fibers, making them more easily pulverized into micron-sized powder. From this process of crushing raw hemp fiber, it was clear that the original residual hemp fiber was solid and challenging to overcome, making a powder with this method. On the other hand, as shown in Figure 2 (a), sulfuric acid breaks down the cellulose fibers into smaller particles. One of the most common chemical treatments is acid hydrolysis. Sulfuric acid can effectively penetrate the cellulose structure of hemp at high concentrations, disrupting the orderly stacking of molecular chains and breaking hydrogen bonds within cellulose [28]. The essence of using sulfuric acid to obtain nanocellulose is to break the 1-4 glycosidic bonds between cellulose macromolecules and remove the amorphous regions of cellulose [29].H+ generated by sulfuric acid damages glycosidic linkages in cellulose macromolecules during acid treatment and heating at 200°C. Since glycosidic linkages are acetals, they become unstable when exposed to high temperatures and acids. Acting as a catalyst, the acid can lower the activation energy of glycoside bonds and accelerate the hydrolysis of cellulose. Due to hydrolysis, cavities were formed on the fiber's surface, as shown in the SEM images, resulting in reduced surface light reflection. As a result, the luster of the thread was soft and the strength low [30,31]. Also, the crusher rotates at three high speeds blades. Weak in hemp fiber strength, hemp fibers break down and become fine under mechanical conditions. Actions including pressure, torsion, and force Between soft fibers and three different types of blade friction, as shown in Figure 1. As a result, the sample was crushed smoothly and became finer, as presented in Figure 3. (b).

Preprints (www.preprints.org) | NOT PEER-REVIEWED | Posted: 28 December 2023 doi:10.20944/preprints202312.2166.v1

4. Crystallinity of Hemp Fiber and Powder

Normalized XRD patterns of OHF, MHF, THF, and HP are presented in Figure 6 (a). The dispersion peak of OHF is maximum at about 22.5° and low is 16.3°. After sulfuric acid treatment MHF showed new heights at 14.8 °and 22.5 °appeared and much weaker. This demonstrates the modification in the crystalline area. After 200°C temperature THF and crushed Hemp powder HP graph showed peaks 14.70° and 22.5°compared to OHF, and MHF was low. Therefore, the four samples showed peaks at around 14.70°, 14.80°, 16.30° and 22.5°. Different crystal faces have other properties, such as hydrophilicity, hydrogen bonding and interfacial interactions. There are four possible crystal faces for cellulose (100), (110), (1bar [28]0)), and (010) [32]. The calculated CI based on peak intensity ratio, the OHF, MHF, THF, and HP crystallinities were 59.65%,89.55%,79.37% and 78.81%, respectively. MHF showed high crystallinity. Higher CI values indicate higher order and alignment of cellulose chains, which may result in higher mechanical strength, thermal stability, and biodegradability of hemp fibers [19,33]. It can be deduced that hydrous ions first attacked the cellulose molecules on their surface before penetrating the easily reactive amorphous area. The hydrolysis of the amorphous region was made worse by the acid's impact. While it may also etch crystallites, the amorphous zone is more affected. Therefore, the hydrolysis of the undeveloped area often improved the crystallinity [34,35]. On the other hand, Crushing rollers can produce cleaner fibers when hemp is spun at more than 400 rpm, resulting from finer particles of whole bran [36]. Using High-speed 25000 r/min crushing, and alkali treatment produced a decrease in HP crystallinity. The crusher can have a small crystallite size, significantly reducing the crystalline fraction. Given that the hemp fiber is crushed and progressively gets the combined pressures of shear and compression mostly destroys shorter, crystalline structures. It concluded that the fine. Therefore, it can be assumed that with a similar crushing process, High-speed crushing also mainly reduces Fiber crystallinity.

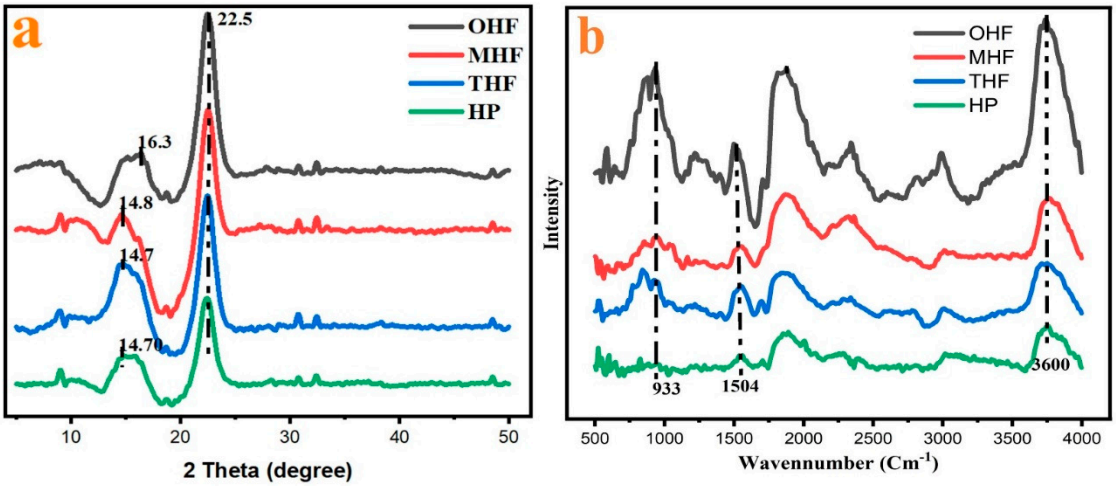

Figure 6. (a) XRD and (b) FTIR result of original hemp fiber (OHF), modified hemp fiber (MHF), temperature hemp fiber (THF), and hemp powder (HP).

4.1. Powder Particle Size and Surface Area

$$(D)=\left(\frac{1}{\sqrt{2\pi}\sigma D}\right) exp\left[-\frac{In^2\left(\frac{D}{D\sigma}\right)}{2\sigma^2}\right] \quad (2)$$

where σD is the standard deviation, and D is the mean particle size. Figure 7(a) shows an example of a typical fitting of the log-normal distribution function to the particle size distribution histogram in the annealed sample [37] . After manually calculating the sizes of the powders' particles using SEM pictures, the average particle sizes were 10 .44μm and the standard deviation was 1.20, statistically evaluated using histograms. The XL-06B at crushing time was 3 to 5 minutes. Friction and shearing forces were applied randomly to the powder because of the high speed and pressure. Figure 7 (a)

Preprints (www.preprints.org) | NOT PEER-REVIEWED | Posted: 28 December 2023 doi:10.20944/preprints202312.2166.v1

shows how uneven and rough the powder surfaces are. Most powder particles have a triangular shape and size of roughly 10%,30%,20%16.7% and 23.3%, respectively.

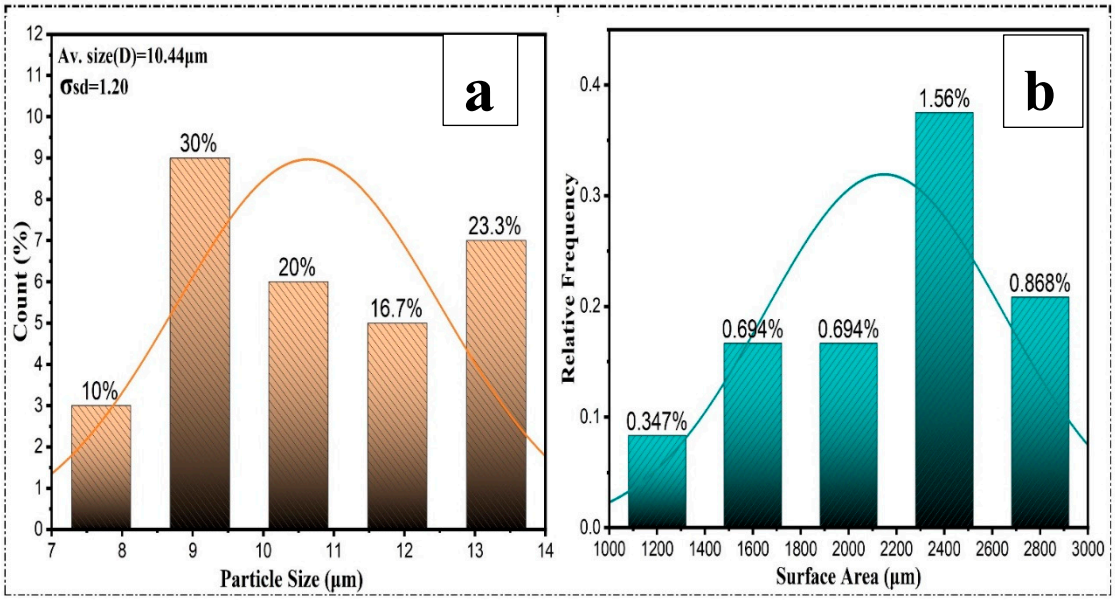

Figure 8. Particle size (μm) a, and Surface area (μm) b.

4.2. Composition Characterization of the Hemp Powder and Fiber

The FTIR spectra in Figure 6 (b) have been normalized for better analysis of chemical modification of modified hemp fiber and powder. Generally, all four curves present similar peak positions; this means after some characteristic group changes, Alkalinity changes, temperature, and crushing process the peaks at 933cm^{-1},1504cm^{-1}and 3734cm^{-1}. The main components of hemp fiber are cellulose and hemicellulose. Corresponding to C–O,C= C and hydroxyl groups O–H strong bonds, respectively, During hydrolysis, the β-1,4-glycosidic link is broken through the cellulose process, which has little impact on the strength of the C-O and O–H bonds [8]. Cellulose is a polysaccharide, and its high chemical reactivity is reached for three reasons Hydroxyl group O-H, which causes high tendency during crosslinking chemical change [2]. High crystalline cellulose is not easily hydrolyzed, while hemicellulose has a low energy, random, amorphous structure. With cellulose, hemicellulose Microfibrils cross-link to attach to cellulose, which makes up around 20% of plant biomass [38]. MHF and THF showed a slight change curve. OHF indicates that the chemical composition and temperature of the hemp fiber have changed after modification. The reaction is the hydrolysis of cellulose in hemp fiber, which breaks the glycosidic bonds between glucose units and produces nanocellulose, a nanomaterial with improved properties [28]. Also, the intensities of the four peaks are significantly reduced after modification.

5. Conclusions

The sulfuric acid modified the leftover hemp cellulose. YK agent to aid dilution into the fiber. Using SEM AFM and XRD pictures, the hemp fibers surface. After treatment, it became rougher, and after 200 ℃, it became significantly harsher. Crushing into hemp powder, the modified hemp fiber's crystallinity increases significantly and decreases after the powder. According to FTIR, the modified fiber substantially decreased strength and was more easily crushed than the original untreated hemp fiber. Eventually, a laboratory crusher produced approximately 1 kg of dry powder with a particle size of 10.44μm in 3 to 5 minutes. This work presents a more efficient method of crushing hemp cellulose fibers into micron-sized dry powders. It could decrease the time and cost of producing cellulose powder while promoting the utilization of cellulose powder across various industries.

Author Contributions: Conceptualization, S.M.S. and S.Z.; methodology, S.M.S; software, S.M.S; investigation, L.G; resources, S.Z.; data curation, L.G.; writing—original draft preparation, S.M.S; writing—review and editing, S.M.S; visualization, Y.H.; supervision, S.Z.

Conflicts of Interest: The authors declare that They have no known competing financial interests or personal relationships could have influenced any work reported in this research paper.

References

1. E. M. Wimalasiri *et al.*, "A framework for the development of hemp (Cannabis sativa L.) as a crop for the future in tropical environments," *Industrial Crops and Products,* vol. 172, p. 113999, 2021/11/15/ 2021, doi: https://doi.org/10.1016/j.indcrop.2021.113999.
2. M. Zimniewska, "Hemp fiber properties and processing target textile: A review," *Materials,* vol. 15, no. 5, p. 1901, 2022.
3. S. Rachel Jacob, A. Mishra, M. Kumari, K. Bhatt, V. Gupta, and K. Singh, "A quick viability test protocol for hemp (Cannabis sativa L.) seeds," *Journal of Natural Fibers,* vol. 19, no. 4, pp. 1281-1286, 2022.
4. M. El Wazna, M. El Fatihi, A. El Bouari, and O. Cherkaoui, "Thermo physical characterization of sustainable insulation materials made from textile waste," *Journal of Building Engineering,* vol. 12, pp. 196-201, 2017.
5. W. Leal Filho *et al.*, "A review of the socio-economic advantages of textile recycling," *Journal of Cleaner Production,* vol. 218, pp. 10-20, 2019.
6. S. Yousef, M. Tatariants, M. Tichonovas, Z. Sarwar, I. Jonuškienė, and L. Kliucininkas, "A new strategy for using textile waste as a sustainable source of recovered cotton," *Resources, Conservation and Recycling,* vol. 145, pp. 359-369, 2019.
7. W. Xu, W. Cui, W. Li, and W. Guo, "Development and characterizations of super-fine wool powder," *Powder Technology,* vol. 140, no. 1-2, pp. 136-140, 2004.
8. L. Gan *et al.*, "Dyeing and characterization of cellulose powder developed from waste cotton," *Polymers,* vol. 11, no. 12, p. 1982, 2019.
9. R. Holdich, *Fundamentals of particle technology*. MidlandIT, 2020.
10. J. Sheng and J. Limei, "Damping properties and micro-morphology of textile waste rubber powder-AO 2246 composites," *Journal of Composite Materials,* vol. 50, no. 7, pp. 963-970, 2016.
11. A. Korpela and H. Orelma, "Manufacture of fine cellulose powder from chemically crosslinked kraft pulp sheets using dry milling," *Powder Technology,* vol. 361, pp. 642-650, 2020.
12. G. Wen, J. Rippon, P. Brady, X. Wang, X. Liu, and P. Cookson, "The characterization and chemical reactivity of powdered wool," *Powder Technology,* vol. 193, no. 2, pp. 200-207, 2009.
13. R. Rajkhowa, Q. Zhou, T. Tsuzuki, D. A. Morton, and X. Wang, "Ultrafine wool powders and their bulk properties," *Powder Technology,* vol. 224, pp. 183-188, 2012.
14. A. T. M. F. Ahmed, M. Z. Islam, M. S. Mahmud, M. E. Sarker, and M. R. Islam, "Hemp as a potential raw material toward a sustainable world: A review," *Heliyon,* vol. 8, no. 1, p. e08753, 2022/01/01/ 2022, doi: https://doi.org/10.1016/j.heliyon.2022.e08753.
15. A. G. Hassabo, M. Salama, A. L. Mohamed, and C. Popescu, "Ultrafine wool and cotton powder and their characteristics," *Journal of natural fibers,* vol. 12, no. 2, pp. 141-153, 2015.
16. Y. He, M. Wan, Z. Wang, X. Zhang, Y. Zhao, and L. Sun, "Fabrication and characterization of degradable and durable fluoride-free super-hydrophobic cotton fabrics for oil/water separation," *Surface and Coatings Technology,* vol. 378, p. 125079, 2019.
17. R. De Silva and N. Byrne, "Utilization of cotton waste for regenerated cellulose fibers: Influence of degree of polymerization on mechanical properties," *Carbohydrate polymers,* vol. 174, pp. 89-94, 2017.
18. M. Kazemimostaghim, R. Rajkhowa, and X. Wang, "Comparison of milling and solution approach for the production of silk particles," *Powder Technology,* vol. 262, pp. 156-161, 2014.
19. S. Park, J. O. Baker, M. E. Himmel, P. A. Parilla, and D. K. Johnson, "Cellulose crystallinity index: measurement techniques and their impact on interpreting cellulase performance," *Biotechnology for Biofuels,* vol. 3, no. 1, p. 10, 2010/05/24 2010, doi: 10.1186/1754-6834-3-10.
20. S. Wu, S. Shi, R. Liu, C. Wang, J. Li, and L. Han, "The transformations of cellulose after concentrated sulfuric acid treatment and its impact on the enzymatic saccharification," *Biotechnology for Biofuels and Bioproducts,* vol. 16, no. 1, p. 36, 2023/03/04 2023, doi: 10.1186/s13068-023-02293-4.
21. L. Gan *et al.*, "Efficient preparation of ultrafine powder from waste cellulose by physicochemical method," *Powder Technology,* vol. 379, pp. 478-484, 2021.

22. A. Shahzad, "A Study in Physical and Mechanical Properties of Hemp Fibres," *Advances in Materials Science and Engineering,* vol. 2013, p. 325085, 2013/08/26 2013, doi: 10.1155/2013/325085.
23. P. K. Gupta *et al.*, "An update on overview of cellulose, its structure and applications," *Cellulose,* vol. 201, no. 9, p. 84727, 2019.
24. J. T. Mhlongo, Y. Nuapia, B. Tlhaole, O. T. Mahlangu, and A. Etale, "Optimization of Hemp Bast Microfiber Production Using Response Surface Modelling," *Processes,* vol. 10, no. 6, p. 1150, 2022. [Online]. Available: https://www.mdpi.com/2227-9717/10/6/1150.
25. K. Rani, M. Ahirwar, and B. K. Behera, "Comparative Analysis of Alkaline and Enzymatic Degumming Process of Hemp Fibers," *Journal of The Institution of Engineers (India): Series E,* vol. 101, no. 1, pp. 1-10, 2020/06/01 2020, doi: 10.1007/s40034-019-00156-y.
26. L. Kuutti, J. Peltonen, J. Pere, and O. Teleman, "Identification and surface structure of crystalline cellulose studied by atomic force microscopy," *Journal of Microscopy,* vol. 178, no. 1, pp. 1-6, 1995.
27. M. A. Torlopov, I. S. Martakov, V. I. Mikhaylov, Y. A. Golubev, P. A. Sitnikov, and E. V. Udoratina, "A Fenton-like system (Cu (II)/H2O2) for the preparation of cellulose nanocrystals with a slightly modified surface," *Industrial & Engineering Chemistry Research,* vol. 58, no. 44, pp. 20282-20290, 2019.
28. V. A. Barbash, O. V. Yushchenko, O. S. Yakymenko, R. M. Zakharko, and V. D. Myshak, "Preparation of hemp nanocellulose and its use to improve the properties of paper for food packaging," *Cellulose,* vol. 29, no. 15, pp. 8305-8317, 2022/10/01 2022, doi: 10.1007/s10570-022-04773-6.
29. M. Ioelovich, "Study of cellulose interaction with concentrated solutions of sulfuric acid," *International Scholarly Research Notices,* vol. 2012, 2012.
30. L. Gan, Z. Xiao, H. Pan, W. Xu, Y. Wang, and X. Wang, "Efficiently production of micron-sized polyethylene terephthalate (PET) powder from waste polyester fiber by physicochemical method," *Advanced Powder Technology,* vol. 32, no. 2, pp. 630-636, 2021.
31. T. Chen, W. Zhang, and J. Zhang, "Alkali resistance of poly (ethylene terephthalate)(PET) and poly (ethylene glycol-co-1, 4-cyclohexanedimethanol terephthalate)(PETG) copolyesters: The role of composition," *Polymer Degradation and Stability,* vol. 120, pp. 232-243, 2015.
32. L. M. J. Kroon-Batenburg and J. Kroon, "The crystal and molecular structures of cellulose I and II," *Glycoconjugate Journal,* vol. 14, no. 5, pp. 677-690, 1997/07/01 1997, doi: 10.1023/A:1018509231331.
33. A. D. French and M. Santiago Cintrón, "Cellulose polymorphy, crystallite size, and the Segal Crystallinity Index," *Cellulose,* vol. 20, no. 1, pp. 583-588, 2013/02/01 2013, doi: 10.1007/s10570-012-9833-y.
34. H. Zhang *et al.*, "Extraction and comparison of cellulose nanocrystals from lemon (Citrus limon) seeds using sulfuric acid hydrolysis and oxidation methods," *Carbohydrate Polymers,* vol. 238, p. 116180, 2020/06/15/ 2020, doi: https://doi.org/10.1016/j.carbpol.2020.116180.
35. P. M. Kibasomba *et al.*, "Strain and grain size of TiO2 nanoparticles from TEM, Raman spectroscopy and XRD: The revisiting of the Williamson-Hall plot method," *Results in Physics,* vol. 9, pp. 628-635, 2018/06/01/ 2018, doi: https://doi.org/10.1016/j.rinp.2018.03.008.
36. M. Baker *et al.*, "Hemp fiber decortications using a planetary ball mill," *Canadian Biosystems Engineering,* vol. 52, no. 2, pp. 2.7-2.15, 2010.
37. S. K. Paswan *et al.*, "Optimization of structure-property relationships in nickel ferrite nanoparticles annealed at different temperatures," *Journal of Physics and Chemistry of Solids,* vol. 151, p. 109928, 2021/04/01/ 2021, doi: https://doi.org/10.1016/j.jpcs.2020.109928.
38. L. J. Gibson, "The hierarchical structure and mechanics of plant materials," *Journal of the Royal Society Interface,* vol. 9, no. 76, pp. 2749-2766, 2012.